REGULAR ARTICLE

Expression of *Slug* in S100β-protein-positive cells of postnatal developing rat anterior pituitary gland

Kotaro Horiguchi[2,3] · Ken Fujiwara[4] · Takehiro Tsukada[4] ·
Hideji Yako[5] · Kozue Tateno[2] · Rumi Hasegawa[2] · Shu Takigami[2] ·
Shunji Ohsako[2] · Takashi Yashiro[4] · Takako Kato[3] · Yukio Kato[1,3,5]

Abstract Among heterogeneous S100β-protein-positive (S100β-positive) cells, star-like cells with extended cytoplasmic processes, the so-called folliculo-stellate cells, envelop hormone-producing cells or interconnect homophilically in the anterior pituitary. S100β-positive cells are known, from immunohistochemistry, to emerge from postnatal day (P) 10 and to proliferate and migrate in the parenchyma of the anterior pituitary with growth. Recent establishment of S100β-GFP transgenic rats expressing specifically green fluorescent protein (GFP) under the control of the *S100β*-promoter has allowed us to observe living S100β-positive cells. In the present study, we first confirmed that living S100β-positive cells in tissue cultures of S100β-GFP rat pituitary at P5 were present prior to P10 by means of confocal laser microscopy and that they proliferated and extended their cytoplasmic processes. Second, we examined the expression of the Snail-family zinc-finger transcription factors, *Snail* and *Slug*, to investigate the mechanism behind the morphological changes and the proliferation of S100β-positive cells. Interestingly, we detected *Slug* expression in S100β-positive cells and its increase together with development in the anterior pituitary. To analyze downstream of SLUG in S100β-positive cells, we utilized specific small interfering RNA for *Slug* mRNAs and observed that the expression of *matrix metalloprotease* (*Mmp*) *9*, *Mmp14* and chemokine *Cxcl12* was down-regulated and that morphological changes and proliferation were decreased.

✉ Kotaro Horiguchi
kota@ks.kyorin-u.ac.jp

✉ Yukio Kato
yukato@isc.meiji.ac.jp

1 Department of Life Science, School of Agriculture, Meiji University, 1-1-1 Higashi-mita, Tama-ku, Kawasaki, Kanagawa 214-8571, Japan

2 Laboratory of Anatomy and Cell Biology, Department of Health Sciences, Kyorin University, 476 Miyashita-cho, Hachioji, Tokyo 192-8508, Japan

3 Institute of Reproduction and Endocrinology, Meiji University, Kanagawa, Japan

4 Division of Histology and Cell Biology, Department of Anatomy, Jichi Medical University School of Medicine, Tochigi, Japan

5 Division of Life Science, Graduate School of Agriculture, Meiji University, Kanagawa, Japan

Thus, our findings suggest that S100β-positive cells express *Slug* and that its expression is important for subsequent migration and proliferation.

Abbreviations

S100β-positive	S100β-protein-positive
GFP	Green fluorescent protein
MMP	Matrix metalloprotease
SNAIL	Snail-family zinc-finger transcription factor Snai1
SLUG	Snail-family zinc-finger transcription factor Snai2
siRNA	Small interfering RNA
BrdU	5-Bromo-2′-deoxyuridine
HE	Hematoxylin and eosin

Introduction

The anterior pituitary (adenohypophysis) consists in the anterior and intermediate lobes. The anterior lobe is composed of five types of hormone-producing cells, S100β-protein-positive cells (S100β-positive cells) and fenestrated sinusoids (i.e., endothelial cells and pericytes). S100β-positive cells were first found in the brain (Moore 1965) and thereafter in several tissues. In the anterior pituitary, S100β-positive cells exhibit a star-like appearance with an extended cytoplasmic process enveloping hormone-producing cells or are interconnected homophilically by E-cadherin in the anterior lobe (Soji et al. 1997; Kikuchi et al. 2006) and are usually referred to as folliculo-stellate cells (Soji et al. 1997). Some of the S100β-positive cells have been suggested to act as stem cells, phagocytes, or regulatory cells for hormone release in the anterior lobe (Inoue et al. 1999; Allaerts and Vankelecom 2005). Based on these histological and physiological features, S100β-positive cells have often been discussed as functionally heterogeneous subpopulations (Allaerts et al. 1996). This heterogeneity has been supported by the observation of different markers occurring in each of the four subpopulations: SOX2 or/and PROP1 (stem/progenitor cell-like; Yoshida et al. 2009, 2011), together with glial fibrillary acidic protein or/and vimentin (astrocyte-like; Tachibana and Yamashima 1988). Moreover, another portion contains keratin (epithelial cell-like; Höfler et al. 1984) or interleukin-6 (IL-6; dendritic cell-like; Horiguchi et al. 2014).

Itakura et al. (2007) succeeded in generating an S100β-GFP transgenic rat strain that expresses green fluorescent protein (GFP) under the control of the S100β-promoter specifically in S100β-positive cells. Using anterior lobes of the S100β-GFP rat, we obtained GFP-positive cell fractions (S100β-positive cell fractions) with a cell sorter and tested their characteristics in primary culture (Horiguchi et al. 2010). We demonstrate that S100β-positive cells are grouped into two types according to their morphological changes under the influence of laminin (Horiguchi et al. 2010, 2014). One has flattened and extended cytoplasmic processes (process type) and the other has a round shape (round type). Recently, by means of their tendency to adhere to the extracellular matrix, we developed a novel and simple method for separating round type cells from process type cells and revealed that the round type is a dendritic cell-like population of S100β-positive cells (Horiguchi et al. 2014). On the other hand, process type S100β-positive cells show a characteristic gene-expression profile with matrix metalloproteinase (*Mmp*)-9, *Mmp*-14 and chemokine *Cxcl12*. Their expression induces the extension of cytoplasmic processes, migration, homophilic interconnection and proliferation (Horiguchi et al. 2012, 2014; Ilmiawati et al. 2012). In the developing anterior lobe, S100β-positive cells appear first along the marginal cell layer encircling the residual lumen at postnatal day (P) 10 (Soji et al. 1997). With age, they increase in number and migrate into the parenchyma with the extension of cytoplasmic processes in a number of directions. However, both the way that S100β-positive cells regulate the expression levels of *Mmps* and *Cxcl12* and the manner in which they proliferate and migrate into the anterior lobe during development remain unclear. To identify the mechanism behind the migration and proliferation of S100β-positive cells at the early postnatal stage, the present study focuses on the expression of Snail-family zinc-finger transcription factors Snail (*Snai1*) and *Slug* (*Snai2*), which are known to induce pronounced cell migration and division during development and which are also considered to be key regulators for the down-regulation of *E-cadherin* and the up-regulation of *Mmps* and *Cxcl12* (Nieto 2002). We demonstrate the expression of *Snail* family transcription factors in S100β-positive cells and evaluate their roles in morphological changes and proliferation. Our findings here indicate that S100β-positive cells express *Slug* and that its expression evokes the morphological changes and proliferation in the postnatal developing anterior lobe.

Materials and methods

Animals and tissue preparation

Transgenic S100β-GFP rats that express GFP under control of the promoter of *S100β*, a marker of folliculo-stellate cells, were provided to us by Professor K. Inoue of Saitama University and bred in our laboratory. Normal adult Wistar rats were purchased from Japan SLC (Shizuoka, Japan). The date of birth was designated as P0. The rats were breast-fed by their mothers until

P20 and then given *ad libitum* access to food and water. They were housed under conditions of 12 h light and 12 h darkness. Rats were killed by exsanguination from the right atrium under deep Nembutal anesthesia and were then perfused with Hanks' balanced salt solution (Life Technologies, Carlsbad, Calif., USA) for culture or with 4 % paraformaldehyde in 50 mM phosphate buffer (pH 7.4) for hematoxylin and eosin staining (HE staining) and immunohistochemistry. The present study was approved by the Committee on Animal Experiments of the School of Agriculture, Meiji University and by the Kyorin University, based on NIH Guidelines for the Care and Use of Laboratory Animals.

Ex vivo slice preparation

The pituitaries of S100β-GFP rats (P5) were dissected and embedded in 4 % agarose (Sigma–Aldrich, St. Louis, Mo., USA) for sectioning at a thickness of 200 μm in the frontal plane. Slices intended for use in time-lapse imaging were individually placed in collagen type I gel (Nitta Gelatin, Osaka, Japan) on 8-well glass chamber slides (1 cm^2/well; Nalge Nunc International, Rochester, N.Y., USA) prior to culture. Slices were then covered with Medium 199 with Earle's salts (Life Technologies) supplemented with 10 % fetal bovine serum (Sigma–Aldrich), 0.5 U/ml penicillin and 0.5 μg/ml streptomycin (Life Technologies).

Time-lapse observation of tissue culture

The sliced tissues were cultured in a CO_2 gas culture chamber with a thermostat (IX3W, Olympus, Tokyo, Japan) installed on a confocal laser microscope (FV1200, Olympus) for 65 h at 37 °C in a humidified atmosphere of 5 % CO_2 and 95 % air. Time-lapse recording of the slices was performed by using a digital camera and software (DP80, Olympus).

Isolation of round and process types of S100β-positive cells

Dispersed cells of the anterior lobe of male S100β-GFP rats (P60) were separated into GFP-positive (mixture of round and process type S100β-positive cells) and GFP-negative cells by a cell sorter (MoFlo XDP, Beckman Coulter, Fullerton, Calif., USA) as described previously (Horiguchi et al. 2014). The GFP-positive cells were cultured on laminin-coated 8-well glass chamber slides for 24 h. Subsequently, the majority of S100β-positive cells showed flattened and markedly extended cytoplasmic processes (process type) but a small number of round type cells were observed. They were removed from the dish with gentle pipetting followed by replacement with fresh medium to the remaining cells. The removed round type cells were collected by centrifuge from the retrieved medium and cultured again in fresh medium for 24 h.

Quantification of mRNA levels by real-time polymerase chain reaction

Total RNA fractions were prepared as described previously (Horiguchi et al. 2011a, 2011b). From 100 ng RNAs, cDNAs were synthesized in 20 μl by a Superscript III reverse transcription (RT) kit with oligo-(dT)$_{20}$ primer (Life Technologies). Quantitative real-time polymerase chain reaction (PCR; ABI PRISM 7500Fast; Life Technologies) was performed with gene-specific primers and the Power SYBR Green PCR Master Mix (Life Technologies). Sequences of the gene-specific primers are listed in Table 1. For normalization, we also quantified β-actin (*b-actin*). The relative gene expression was calculated by comparing the cycle times for each target PCR. Cycle threshold values were converted to relative gene expression levels by using the $2^{-(\Delta Ct\ sample-\Delta Ct\ control)}$ method.

Immunohistochemistry

Tissue preparation and immunohistochemistry were performed as described previously (Horiguchi et al. 2014). Frozen frontal sections (8 μm thick; taken at P5, P10 and P60) were obtained by using a cryostat (Tissue-tek polar DM; Sakura Finetek, Tokyo, Japan) and were mounted on slide glasses. Sections were immersed in 0.5 % Triton X-100 with phosphate-buffered saline (PBS) and incubated in PBS containing 2 % normal goat serum for 20 min at 30 °C. They were then incubated overnight with mouse anti-rat SLUG polyclonal antibody (1:100; Santa Cruz Biotechnology, Santa Cruz, Calif., USA) at room temperature. After being washed with PBS, sections were incubated in PBS with Alexa-Fluor-568-conjugated goat anti-rabbit IgG (Life Technologies) diluted to 1:200 and were washed with PBS again. The sections were then enclosed in mounting medium containing 4′,6-diamino-2-phenylindole (DAPI; Vector Laboratories, Burlingame, Calif., USA) to counterstain nuclei. Absence of an observable nonspecific reaction was confirmed by using normal mouse or rabbit serum. Sections were scanned by using a fluorescence microscope (cellSens Dimension system, Olympus).

Measurement of the number of GFP-positive and SLUG-immunopositive cells

Ten random fields were imaged per anterior pituitary at P5, P10 and P60 by using a fluorescence microscope with a ×60 objective lens. The number of cells positive for GFP and SLUG and the total number of cells per area (105×140 μm square) stained by DAPI were counted by the cellSens Dimension system (Olympus). The observations were performed three times for each experimental group.

Table 1 Primers for real-time polymerase chain reaction (*Snail*, *Slug*, Snail-family zinc-finger transcription factors, *Mmp* matrix metalloproteinase, *Cdh* cadherin, *Cxc* chemokine, *b-actin* β-actin)

Genes	Primer sequence (5′-3′)	Product size	Genbank accession number
Snail	Froward: TGCTCCACAAACACCAAGAG Reverse: TCCCTGGACTTAAGCTGGAA	134	NM_053805
Slug	Forward: CATCTGCAGACCCACTCTGA Reverse: AGCAGCCAGACTCCTCATGT	103	NM_013035
Mmp9	Forward: AGGGTCGGTTCTGACCTTTT Reverse: ATAAAGGGCCGGTAAGGTG	106	NM_031055
Mmp14	Forward: AAGCTTGGCTGCAGCAGTAT Reverse: GCCTTGCCTGTCACTTGTAA	133	NM_031056
Cdh1	Forward: CCCAGGAAATACACCCCTCT Reverse: CACCAACACACCCAGCATAG	127	NM_031334
Cxc112	Forward: GTTTGCTTTGGAGCTTCTCG Reverse: GCTCTGGTGGAAGGTTGCTA	99	NM_022177
Cxcr4	Forward: GCCATGGCTGACTGGTACTT Reverse: GATGAAGGCCAGGATGAGAA	99	NM_022205
S100b	Forward: ATAGCACCTCCGTTGGACAG Reverse: TCGTTTGCACAGAGGACAAG	132	NM_013191
b-actin	Forward: CATTGCTGACAGGATGCAGAAGG Reverse: TGCTGGAAGGTGGACAGTGAGG	138	NM_031144

Immunoblot analysis

Anterior lobes at P5, P10 and P60 were washed in PBS and lysed in RIPA buffer (20 mM TRIS, 150 mM NaCl, 2 mM EDTA, 0.1 % v/v SDS, 1 % v/v Triton X-100, pH 7.5) and total protein concentrations were determined with a bicinchoninic acid (BCA) protein assay kit (Pierce, Rockford, Ill., USA). Protein (10 μg) from each sample was analyzed by 5–20 % gradient SDS-polyacrylamide gel electrophoresis. Molecular weight marker (MagicMark XP Western Protein Standard, Life Technologies) was concomitantly loaded. Proteins were then transferred electrophoretically onto an Immobilon-P transfer membrane (Millipore, Bedford, Mass., USA). The protein was detected as described previously (Horiguchi et al. 2012). The membrane was incubated overnight with rabbit polyclonal SLUG (1:2000; Santa Cruz), rabbit MMP9 (1:3000; LifeSpan BioSciences, Seattle, Wash., USA), rabbit MMP14 (1:1500; Abcam, Cambridge, UK), mouse monoclonal E-cadherin (1:80,000; BD Biosciences, San Jose, Calif., USA), or mouse monoclonal β-actin (0.3 μg/ml; Sigma-Aldrich) antibodies. Each analysis was performed in triplicate. As a negative control, we loaded the sample buffer without a sample and did not observe any bands (data not shown).

Cell culture and small interfering RNA for knockdown of *Slug* mRNA

Dispersed cells were prepared from Wistar rats (P60) as described previously (Horiguchi et al. 2010) by plating them onto 8-well glass chamber slides with and without a laminin-coated surface as described above. Cells were then cultured for 24 h at 37 °C in a humidified atmosphere of 5 % CO_2 and 95 % air. For transfection of small interfering RNA (siRNA), the culture medium was replaced by 400 μl Medium 199 with Earle's salts after 24 h cultivation and supplemented with siRNA against *Slug* mRNA (0.2 μM, Rn_Snai2_1; Qiagen, Valencia, Calif., USA) and transfection reagent (INTERFERin at 1:100 v/v, PolyPlus Transfection, New York, USA). Subsequently, the anterior pituitary cells were cultured for 48 h. A non-silencing siRNA without homology to any known mammalian gene was used as a negative control (Qiagen). After 48 h, cells were incubated with 5 mM EDTA solution for 20 min at 37 °C. The suspended EDTA solution was retrieved and cells were collected by centrifuge and cultured again for 24 h on 8-well glass. We observed the morphological changes in S100β-positive cells by using immunocytochemistry for S100β protein as described below.

Immunocytochemistry

Cultured cells fixed with 4 % paraformaldehyde in 25 mM phosphate buffer for 15 min at room temperature were first immersed in PBS containing 0.5 % Triton X-100 for 5 min at room temperature. Cells were also immersed in 2 % normal goat serum for 20 min at 30 °C and then incubated with anti-rat S100β protein rabbit polyclonal antibody (1:1000; DAKO) overnight at room temperature. After being washed with PBS, cells were incubated in PBS with Alexa-Fluor-488-conjugated goat anti-rabbit IgG diluted to 1:200. Absence of an observable nonspecific reaction was confirmed by using normal rabbit serum.

Proliferation assay

To visualize the proliferative activities of cells, the nucleotide analog 5-bromo-2′-deoxyuridine (BrdU, Sigma–Aldrich) at a concentration of 3 μg/ml was added to the primary culture for 24 h after the addition of siRNA. Cells were fixed in 4 % paraformaldehyde in 25 mM phosphate buffer (pH 7.4) for 20 min at room temperature and were then treated with 4 M HCl in PBS for 10 min. Cells were incubated in PBS containing 2 % normal goat serum for 1 h at 30 °C and were then incubated with anti-rat BrdU mouse monoclonal antibody (1.5 μg/ml, Sigma–Aldrich) and anti-rat S100β protein overnight at room temperature. After being washed with PBS, cells were incubated in PBS with Alexa-Fluor-568-conjugated goat anti-mouse IgG and Alexa-Fluor-488-conjugated goat anti-rabbit IgG (Life Technologies) diluted to 1:200. The absence of an observable nonspecific reaction was confirmed by using normal mouse serum. Ten fields per well were randomly imaged by using a confocal laser microscope with a ×60 objective lens. The immunoreactive cells were counted (at least 100 cells per well) as described previously (Horiguchi et al. 2010, 2011b; Ilmiawati et al. 2012). The observations were performed three times for each experimental group.

Statistical analysis

Data are presented as means±SEM for at least three rat preparations in each group. Student's t-test after the F-test was

Fig. 1 Observation of S100β-positive cells in developing anterior lobe. Hematoxylin and eosin (HE) staining (**a**–**c**) and green fluorescent protein (GFP) images (**d**–**f**) at postnatal (*P*) days 5 (P5, **a**, **d** same sections), 10 (P10, **b**, **e** same sections) and 60 (P60, **c**, **f** same sections) of S100β-GFP male rats (*PL* posterior lobe, *IL* intermediate lobe, *AL* anterior lobe). *Bar* 100 μm. **g** *S100β* mRNA levels in developing anterior lobe were determined by real-time polymerase chain reaction (PCR) and are presented after normalization with an internal control *b-actin* (means±SEM, *n*= 4). *S100β* mRNA levels were calculated as ratios against the P3 value. **h**–**j** Time-lapse images in pituitary tissue culture of S100β-GFP male rat at P5. Time-lapse image tissues were recorded at 15-min intervals under a confocal laser microscope for 65 h after tissues were incubated. A GFP-positive cell (*arrow*) elongated its cytoplasmic processes and migrated. The other cell (**h**, **i**, *arrowheads*) appeared to divide into two cells (**j**, *arrowheads*). The time (h:min:s) that had elapsed from the plating of tissues is shown *lower left*. *Bar* 50 μm
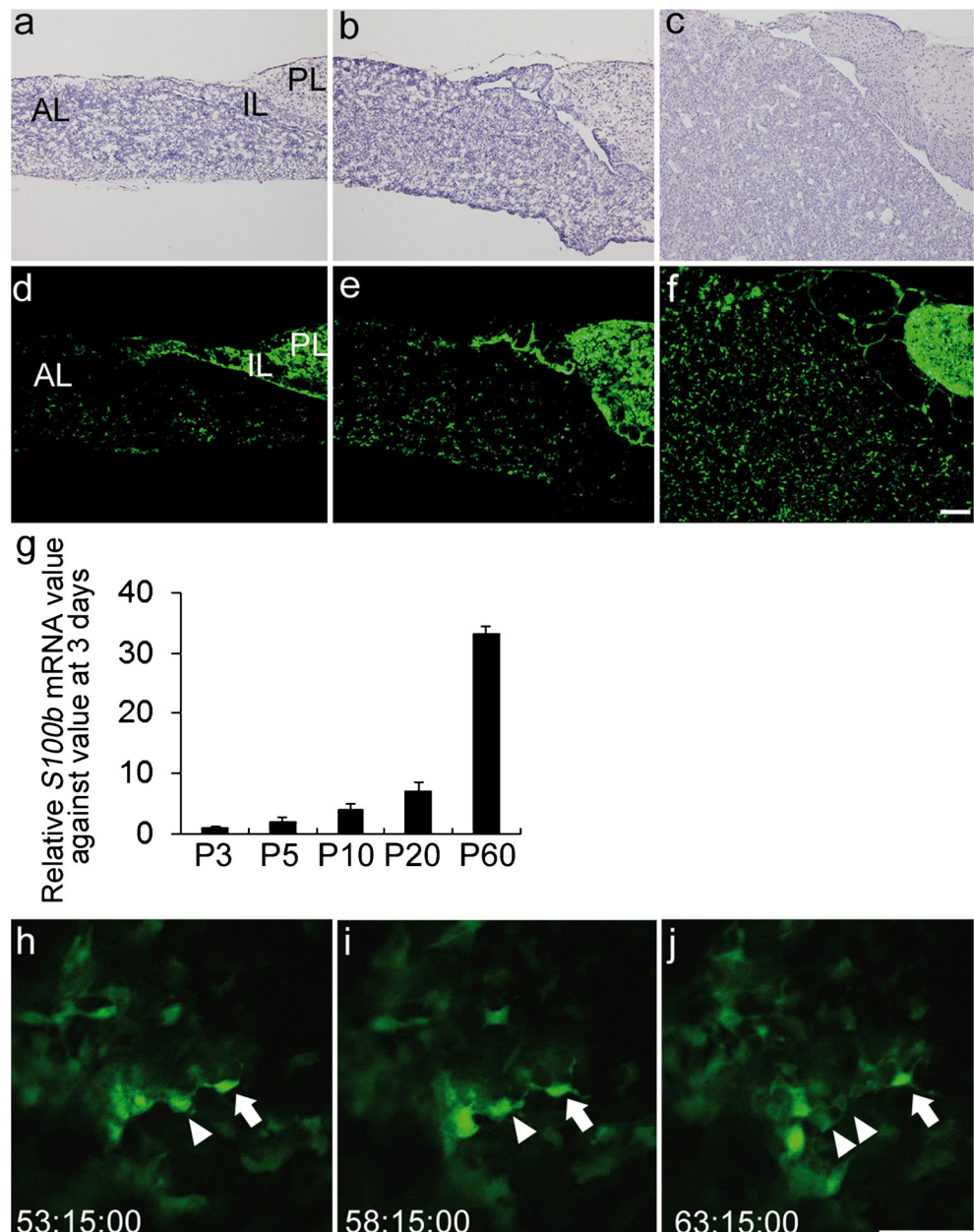
Fig. 2 *Snail*- and *Slug*-mRNA levels in S100β-positive cells of anterior lobe at P60. *Snail*- and *Slug*-mRNA levels were determined by real-time PCR and normalized with an internal control (*b-actin*; means±SEM, *n*=3). **a** *Snail*- and *Slug*-mRNA levels in anterior lobe at P60. **b** Comparison of *Snail*- and *Slug*-mRNA levels in GFP-negative (−) and GFP-positive (+) cells at P60 represented as a ratio to those of GFP-negative cells. **c** Comparison of *Snail*- and *Slug*-mRNA levels at P60 in primary cultures on uncoated (*Un*) and laminin-coated (*Lami*) surfaces represented as a ratio to those cultured on the uncoated surface. **d** Comparison of *Snail*- and *Slug*-mRNA levels in the round (*R*) and process (*P*) type S100β-positive cells at P60 represented as a ratio to those of the round type. *$P<0.05$
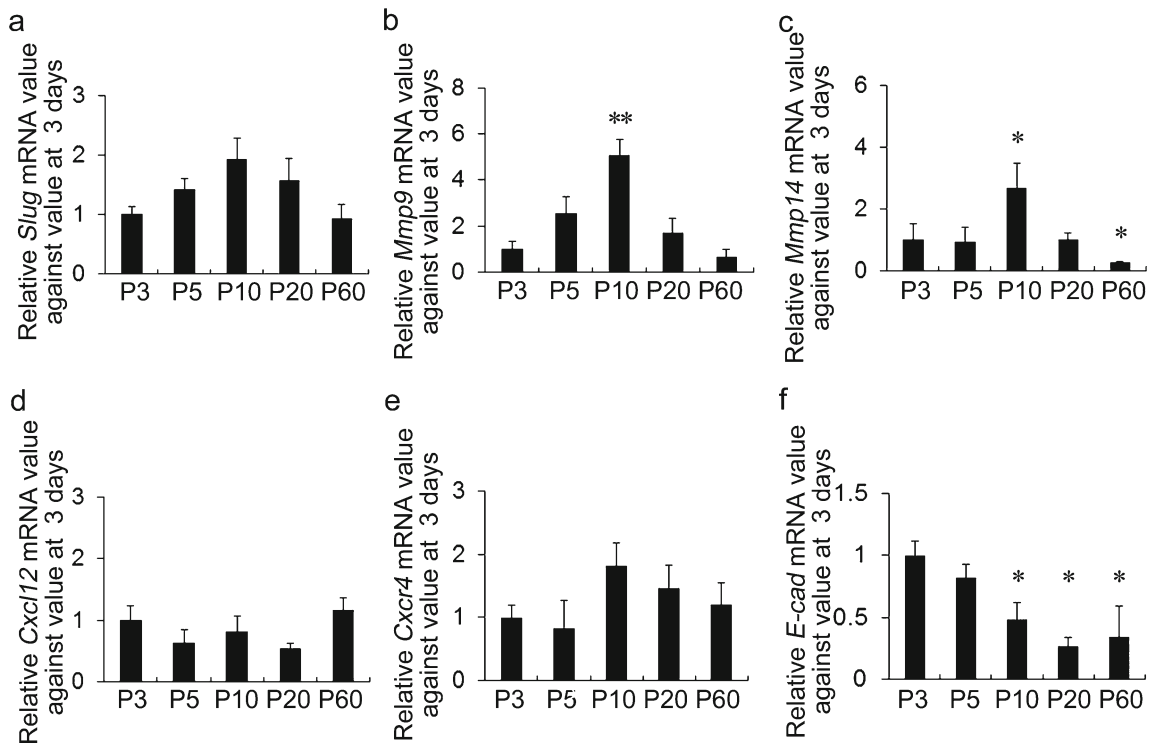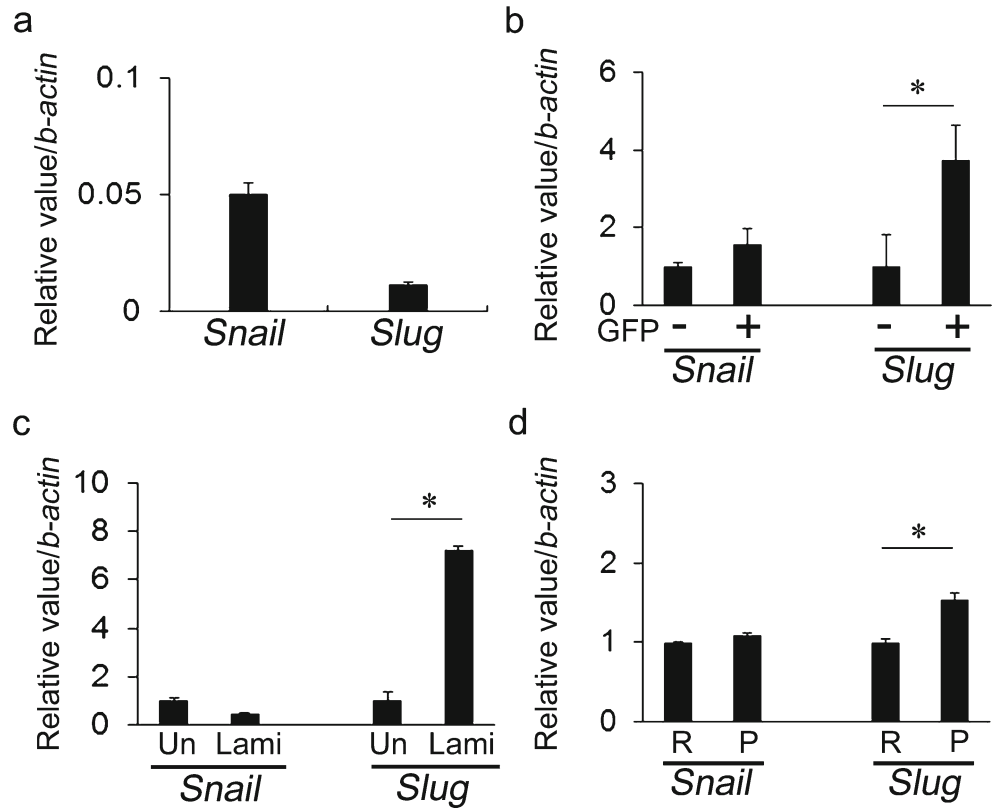

Fig. 3 Expression of *Slug* (**a**), *Mmp9* (**b**), *Mmp14* (**c**), *Cxcl12* (**d**), *Cxcr4* (**e**) and *E-cadherin* (*E-cad*, **f**) during postnatal anterior pituitary development. *Slug*-, *Mmp9*-, *Mmp14*-, *Cxcl12*-, *Cxcr4*- and *E-cad*-mRNA levels in developing anterior lobe (P3, P5, P10, P20 and P60) were determined by real-time PCR and normalized with an internal control *b-actin* (means±SEM, *n*=3). The mRNA levels were calculated as ratios of the value at P3. The significance of differences between the value at P3 and that at other days was determined by the Dunnett's test. ** $P<0.01$, * $P<0.05$

used for two-group comparisons and Dunnett's test or two-tailed multiple *t*-test with Bonferroni correction was used for multiple comparisons. Differences were considered significant when *P* was less than 0.05.

Results

Observation of S100β-positive cells in postnatal developing anterior lobe

HE staining (Fig. 1a–c) and GFP images (Fig. 1d–f) of S100β-GFP rat pituitaries at P5 (Fig. 1a, d), P10 (Fig. 1b, e) and P60 (Fig. 1c, f) are shown. GFP-positive cells in the anterior lobe were confirmed to be S100β-positive cells (Itakura et al. 2007). We reconfirmed the presence of GFP-expressing cells in the anterior lobe at P5 (Fig. 1d) and demonstrated an increase in their number with development (Fig. 1d–f). This was confirmed by real-time PCR analysis of *S100β* mRNA in the developing anterior pituitary (Fig. 1g). Subsequently, observation of living GFP-expressing cells during tissue culture prepared from an S100β-GFP male rat pituitary at P5 was performed. The pituitary slices were cultured in a CO_2 gas culture chamber on a confocal laser microscope and photographed every 15 min for a period of up to 65 h. Typical images demonstrated morphological changes and proliferating cells (Fig. 1h–j, arrows and arrowheads, respectively) within the anterior lobe (see Supplementary Movie 1).

Expression of *Snail* and *Slug* in S100β-positive cells at P60

We performed quantitative real-time PCR for *Snail* and *Slug* mRNAs, which are known to play a role in cell migration, in order to determine whether S100β-positive cells expressed these genes. We first confirmed the expression of *Snail* and *Slug* in anterior pituitary tissue at P60 (Fig. 2a) and then analyzed their expression in GFP-positive or GFP-negative cells prepared by the cell sorter from an S100β-GFP male rat anterior lobe at P60. *Slug* expression was significantly higher (*P*<0.05) in GFP-positive cells than in GFP-negative cells, whereas the levels of *Snail* expression were not significantly different (Fig. 2b). Second, we determined whether *Snail* and *Slug* expression in the primary cultures of S100β-positive cells at P60 were affected by laminin, which had induced the migration and proliferation of S100β-positive cells in previous studies (Horiguchi et al. 2010, 2012). *Slug* expression was significantly higher (*P*<0.05) in S100β-positive cells cultured on the laminin-coated surface for 72 h than in those cultured on the uncoated surface (Fig. 2c). Since S100β-positive cells at P60 are composed of two cell types with different affinities for laminin (Horiguchi et al. 2010, 2014), we also examined their expression in the two subpopulations, i.e., round and

process types of S100β-positive cells. We found that *Slug* expression in the process type was significantly (*P*<0.05) higher (more than twice) than that of the round type (Fig. 2d).

Expression profile of genes related to morphological changes and proliferation in postnatal developing anterior lobe

Soji et al. (1994) demonstrated that S100β-positive cells increase in number, migrate (as they age) to the parenchyma and develop cytoplasmic processes that extend in a number of directions at around P10. We examined the expression of genes related to the migration and proliferation of S100β-positive cells in postnatal development of the anterior lobe by real-time PCR. *Slug*- and *Cxcr4*-mRNA levels tended to increase until P10, followed by a decrease
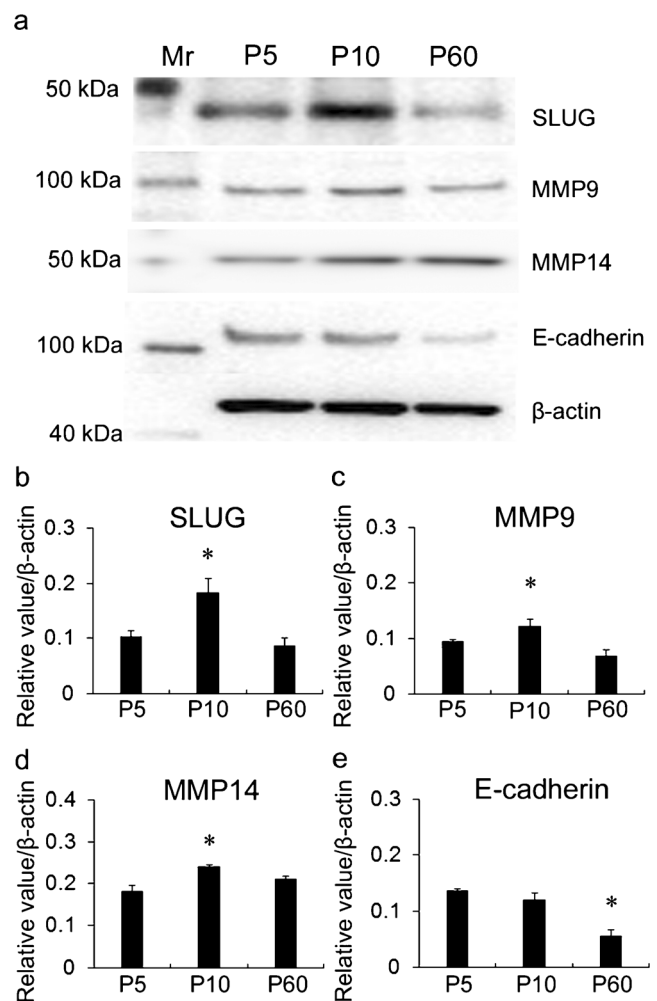
Fig. 4 Western blot analysis of SLUG, MMP9, MMP14 and E-cadherin during postnatal pituitary development. **a** SLUG, MMP9, MMP14 and E-cadherin in developing anterior lobe at P5, P10 and P60 (*Mr* molecular size marker). **b–e** Amounts of SLUG (**b**), MMP9 (**c**), MMP14 (**d**) and E-cadherin (**e**) from three experiments (means±SEM, *n*=3) were quantified by densitometry and normalized with that of β-actin. The significance of the differences was determined by the Bonferroni test. **P* <0.05

thereafter (Fig. 3a, e). *Mmp9*- and *Mmp14*-mRNA levels at P10 were significantly higher than those at P3 (Fig. 3b, c). The *Mmp14*-mRNA level at P60 decreased significantly compared with that at P3 (Fig. 3c). On the other hand, the *Cxcl12*-mRNA level was unchanged (Fig. 3d) and the *E-cadherin*-mRNA level was significantly decreased at P10, P20 and P60 as compared with that at P3 (Fig. 3f). In addition, we examined protein levels for SLUG, MMP9, MMP14 and E-cadherin by immunoblotting of the anterior lobe at P5, P10 and P60. The bands reacted with each antibody in a manner that gave the expected molecular size for each protein (Fig. 4a). When quantitative measurement of the immunoblot analyses was performed by normalization with β-actin, the protein levels of SLUG, MMP9 and MMP14 were highest at P10 among the days examined (Fig. 4b–d). On the other hand, the protein level of E-cadherin was highest at P5 with a decrease in development (Fig. 4e).

Immunohistochemistry of SLUG

Using the anterior lobe of the S100β-GFP rat at P5, P10 and P60, we examined whether S100β-positive cells were positive for SLUG by immunohistochemistry. As shown in Fig. 5, some of the S100β-positive cells at P10 were immunopositive for SLUG (Fig. 5a–d). GFP-positive cells of high fluorescence intensity did not express SLUG (asterisks in Fig. 5a–d). Next,

we counted the number of the S100β-positive cells and SLUG-immunopositive cells per unit area. The total number of cells stained by DAPI was also counted. They decreased with advancing age over days in an inverse proportion to cell size (Fig. 5e). The numbers of GFP-positive cells (S100β-positive cells) and SLUG-immunopositive cells at P60 were also smaller than those at P5 and P10 (Fig. 5e). However, the ratio of SLUG-immunopositive cells and GFP-positive cells at P10 was higher than those at P5 and P60 (Fig. 5e).

Knockdown of *Slug*-mRNA level by siRNA

To evaluate the role of SLUG in the morphological changes and proliferation of S100β-positive cells, we used siRNA to down-regulate the *Slug*-mRNA level in the primary cultures of Wistar rat anterior pituitary cells at P60. When the *Slug*-mRNA level was downregulated with a specific siRNA, it significantly decreased (Fig. 6a). We then performed quantitative analyses for the mRNA levels of *Mmp9*, *Mmp14* and *Cxcl12* in *Slug*-siRNA-treated cells. We observed that their mRNA levels significantly decreased ($P<0.05$) compared with those in the control siRNA-treated cells but *E-cadherin* expression was slightly but significantly higher ($P<0.05$; Fig. 6a). *Cxcr4* expression was not changed in treatments with non-silencing and *Slug*-siRNA (Fig. 6a).
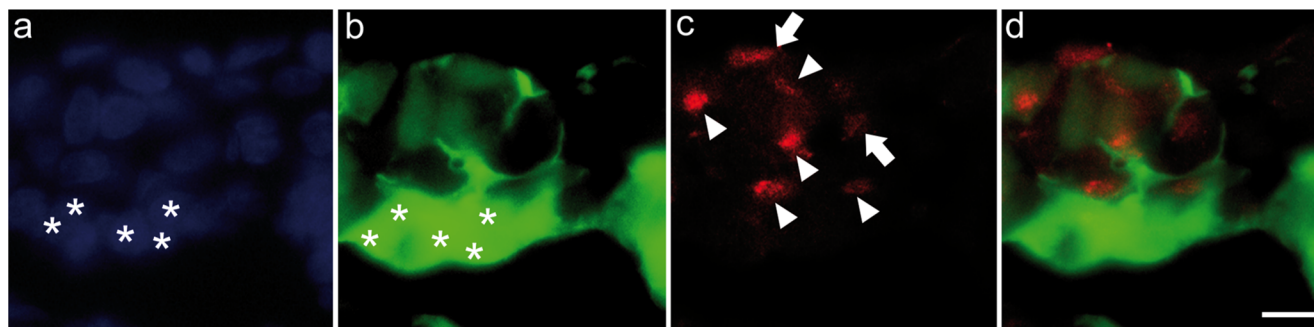

	Total cell number	GFP (GFP/Total cell number (%))	SLUG (SLUG/Total cell number (%))	SLUG/GFP-positive cell number (%)
P5	186.60±6.12	17.88±2.29 (9.67±1.45)	8.76±1.23 (4.74±0.78)	35.45±1.36
P10	*145.11±1.54	15.72±1.28 (10.84±0.9)	7.04±0.86 (4.84±0.55)	*79.96±3.99
P60	*109.96±2.55	*10.33±0.80 (9.39±0.68)	*2.61±0.23 (2.39±0.26)	55.45±1.97

Fig. 5 Immunohistochemistry for SLUG. **a–d** Immunohistochemistry of SLUG in the anterior lobe of S100β-GFP male rats at P10. **a** DAPI (4′,6-diamino-2-phenylindole) staining. **b** GFP image (*asterisks* high fluorescence intensity of GFP-positive cells). **c** Immunoreactivity for SLUG (*arrowheads* cells double-positive for GFP and SLUG, *arrows* SLUG-positive cells but GFP-negative cells). **d** Merged image of **b**, **c**. *Bar* 50 μm. **e** Cell numbers positive for each protein within the field of a ×60 objective lens (105×140 μm square) for three subjects. The proportions of the cell population positive for DAPI (total cell number), for GFP and for SLUG are indicated. The ratio of GFP and SLUG double-positive cells (*SLUG/GFP-positive cell number*) is also indicated. The significance of the differences was determined by the Bonferroni test. *$P<0.05$

Fig. 6 Downregulation of *Slug*-mRNA level by siRNA. **a** *Slug*-, *Mmp9*-, *Mmp14*-, *E-cadherin*- (*E-cad*), *Cxcl12*- and *Cxcr4*-mRNA levels of cells cultured with non-silencing siRNA (*closed bar*) and *Slug*-siRNA (*open bar*) for 48 h were determined by real-time PCR (means±SEM, *n*=3), followed by normalization with an internal control (*b-actin*). **P<0.05*. **b–g** Immunocytochemistry of S100β protein following 24-h incubation after anterior pituitary cells were transfected by siRNA for 48 h and re-plated (**b–d** non-silencing siRNA, **e–g** *Slug*-siRNA). **b, e** Phase-contrast images. **c, f** Immunoreactive S100β protein (*arrows* cytoplasmic processes in S100β-positive cells). **d, g** Merged image of immunoreactive S100β protein and DAPI staining. *Bar* 50 μm
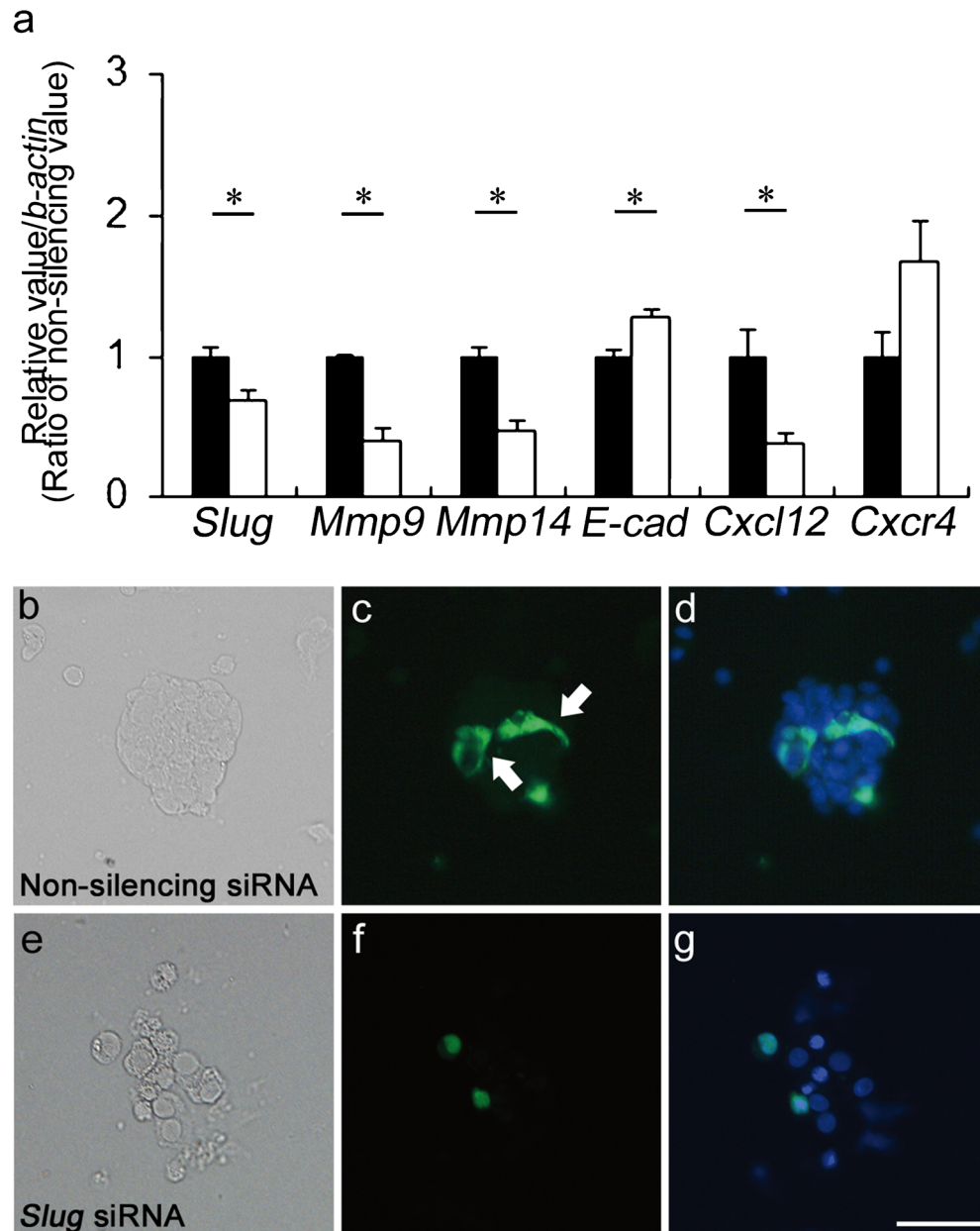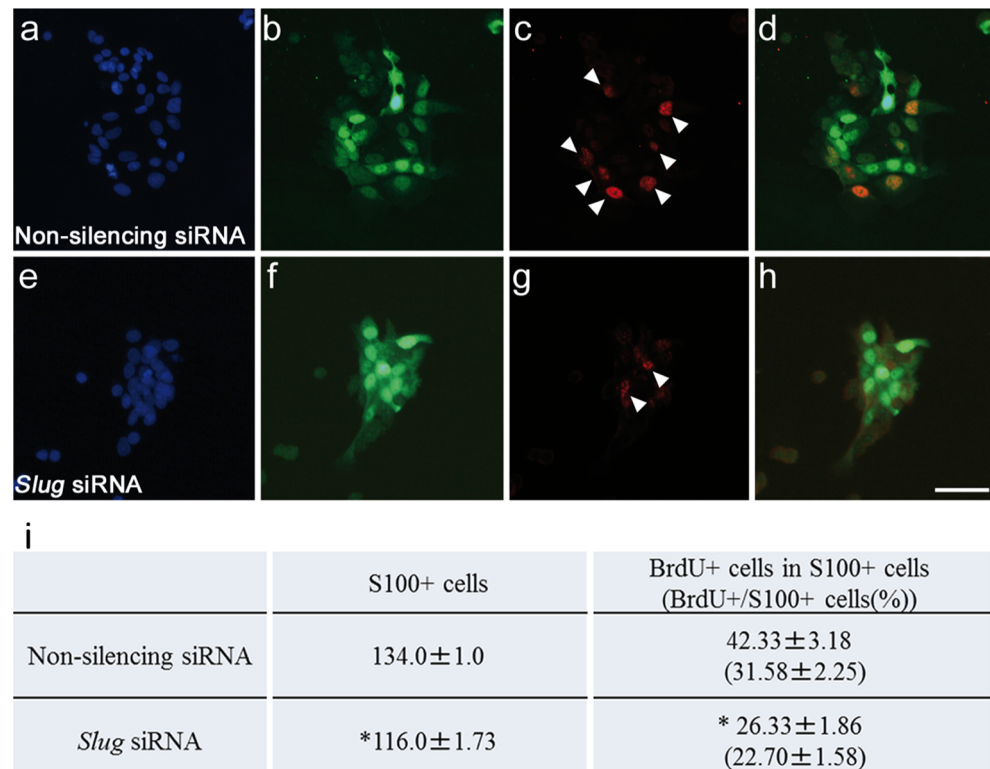

After siRNA treatment for 48 h, we retrieved and re-dispersed anterior pituitary cells on 8-well chamber slides in order to observe the morphological changes of treated S100β-positive cells, followed by a further 24-h culture. Then, we conducted immunocytochemistry of S100β protein and observed that S100β-positive cells treated with control siRNA extended cytoplasmic processes similar to those at the start of culture (Fig. 6b–d), whereas such morphologies were not observed in the cells after *Slug*-siRNA treatment (Fig. 6e–g). In primary culture on laminin-coated surfaces, proliferation of S100β-positive cells was observed frequently from 48 to 72 h after cells were plated (Horiguchi et al. 2010).

Next, we examined whether the knockdown of the *Slug*-mRNA level influenced the proliferation of S100β-positive cells by treatment of the cells with *Slug*-siRNA for 24 h and by labeling with BrdU for another 24 h in the laminin-coated plates, since their proliferation was only observed in coated plates. Morphological observations of immunoreactivity for S100β protein and BrdU in anterior pituitary cells are shown in Fig. 7. Many S100β-positive cells after non-silencing and *Slug*-siRNA treatment had flattened and extended cytoplasmic processes (process type) under the influence of laminin in primary culture (Fig. 7b, f). A number of cells double-positive for S100β protein and BrdU were observed (Fig. 7a–h). The numbers of S100β-positive cells and of S100β protein and BrdU double-positive cells were significantly lower (*P<0.05*) in *Slug*-siRNA-treated cells than in control-siRNA-treated cells (Fig. 7i).

Fig. 7 Effect of *Slug*-siRNA on proliferation of S100-positive cells cultured on a laminin-coated surface. **a–h** Fluorescence microscopy performed with S100-positive cells transfected with siRNA and cultured in BrdU-containing medium to label proliferating cells for 24 h (means ±SEM, *n*=3). **a, e** DAPI staining (*blue*). **b, f** S100β protein (*green* immunofluorescence staining). **c, g** BrdU (*red* immunofluorescence staining, *arrowheads* BrdU-positive cells). **d, h** Merged image of DAPI, S100β protein and BrdU. *Bar* 50 μm. **i** Numbers of S100β-positive cells (*S100+ cells*) and of BrdU-positive cells and S100+ cells (*BrdU+ cells in S100+ cells*) in a microscope field. Differences in numbers with regard to non-silencing siRNA and *Slug*-siRNA were statistically significant (**P*<0.05)

	S100+ cells	BrdU+ cells in S100+ cells (BrdU+/S100+ cells(%))
Non-silencing siRNA	134.0±1.0	42.33±3.18 (31.58±2.25)
Slug siRNA	*116.0±1.73	* 26.33±1.86 (22.70±1.58)

Discussion

In the present study, we succeeded in conducting a time-lapse observation of motile S100β-positive cells by using living tissue slices of the anterior pituitary gland. We also revealed that transcription factor *Slug* is expressed in S100β-positive cells and that the inhibition of its expression impairs the morphological changes and proliferation activity of these cells.

Two decades ago, Soji et al. (1994) observed S100β protein as a marker of folliculo-stellate cells in rat anterior lobe and showed postnatal changes of the localization of these cells by using immunohistochemistry. According to their report, the immunopositive cells with S100β protein are sparse and difficult to identify before P10 and are faintly observed along the marginal cell layer at P10. With age, S100β-positive cells increase in number and their migration into the parenchyma of the anterior lobe was postulated. However, a definite observation of the behavior of S100β-positive cells has yet to be made. The generation of S100β-GFP rats that express GFP under the control of the S100β promoter by Itakura et al. (2007) enabled us to show several characteristics of S100β-positive cells by using their GFP expression including living cell observation (Horiguchi et al. 2010, 2011a, 2011b, 2012, 2014). In the present study, we confirmed the presence of GFP-positive cells in the anterior pituitary prior to P10 by observing living cells. Furthermore, a 65-h time-lapse observation of the anterior pituitary at P5 (Fig. 1h–j, Supplemental

movie 1) revealed images of GFP-positive cells extending cytoplasmic processes and of some of them proliferating in the anterior lobe. We have previously demonstrated that S100β-positive cells are able to differentiate into hormone-producing cells and proliferate in dispersed cell culture (Higuchi et al. 2014). In addition, we have observed that dispersed S100β-positive cells actively migrate and proliferate in cell culture (Horiguchi et al. 2010, 2012). Taken together, the accumulating results suggest that S100β-positive cells may well act as a cell resource by migration and proliferation. Meanwhile, several investigators have shown that the extracellular matrix components are synthesized in the developing anterior lobe at an early stage (Horacek et al. 1993; Ramadhani et al. 2014). We demonstrated that integrin-β1 (receptor of extracellular matrices) of the S100β-positive cells receives signals that lead to morphological changes and proliferation activity (Horiguchi et al. 2011a, 2011b, 2012; Ilmiawati et al. 2012). Accordingly, the morphological changes and proliferation of S100β-positive cells at P5 appear to be supported by the interaction of integrin-β1 signaling and the extracellular matrix.

Snail and *Slug* are members of the Snail family of zinc-finger transcription factors that share an evolutionary conserved role in mesoderm formation in vertebrates (Aybar et al. 2003; Sefton et al. 1998). *Slug* was first identified in the migratory neural crest cells in chick embryo (Nieto et al. 1994) and is an essential factor for gastrulation, epithelial-mesenchymal transition and cell survival (Sanchez-Martin

et al. 2003; Sefton et al. 1998). In the present study, we found that *Slug* is expressed in a subpopulation of S100β-positive cells, namely in the process type cells but not the dendritic-like cells (round type) and have shown morphological changes under the influence of extracellular matrices (Figs. 2, 7). Although further study is necessary to determine the origin of S100β-positive cells in the anterior lobe, these findings lead us to speculate that process type S100β-positive cells have characteristics of neural crest cells.

We observed that the mRNA and protein levels of SLUG, MMP9 and MMP14 in the anterior pituitary have their highest values at P10 (Figs. 3, 4, 5), corresponding to the first growth wave of the pituitary with accompanying migration and proliferation (Soji et al. 1997; Yoshida et al. 2011, 2013). On the other hand, the RT-PCR assay carried out simultaneously showed that the mRNA and protein levels of E-cadherin decreased with age (Figs. 3, 4). The molecules, SLUG, MMP9, MMP14, E-cadherin and CXCL12 analyzed in the present study are known to be involved in cell migration. A series of previous studies (Horiguchi et al. 2011a, 2011b, 2014; Ilmiawati et al. 2012) revealed that MMP9 and MMP14 induce the development of cytoplasmic processes and proliferation under the influence of laminin. We have shown that CXCL12 facilitates the extension and interconnection of cytoplasmic processes and inhibits morphological change via the CXCL12 inhibitor (Horiguchi et al. 2012). Kikuchi et al. (2006) demonstrated that S100β-positive cells interconnect with each other by E-cadherin. However, as is well-known, the factors for cell migration form a cascade beginning with SLUG as an upstream modulator leading to downstream MMP9, MMP14 and E-cadherin (Joseph et al. 2009; Jordà et al. 2005; Shields et al. 2012). To confirm this cascade in S100β-positive cells, we examined *Slug*-siRNA treatment and observed the inhibition of the morphological changes and proliferation of extending cytoplasmic processes of S100β-positive cells (Figs. 6, 7). By real-time PCR in a simultaneous experiment with *Slug*-siRNA, we confirmed the decrease of *Mmp9*-, *Mmp14*- and *Cxcl12*-mRNA levels and the promotion of the *E-cadherin*-mRNA level (Fig. 6), all of which are consistent with previous observations that SLUG promotes *Cxcl12* expression (Uygur and Wu 2011; Piva et al. 2011) and represses *E-cadherin* (Batlle et al. 2000; Bolos et al. 2003). However, *Slug*-siRNA does not induce the inhibition of the *Cxcr4*-mRNA level (Fig. 6a). Consequently, the present data suggest that SLUG enhances the migration and proliferation activity of S100β-positive cells through the up-regulation of MMP9, MMP14 and CXCL12, regardless of CXCR4 and the down-regulation of E-cadherin.

In the present study, we observed the morphological change and proliferation of living S100β-positive cells in the rat anterior lobe at P5, demonstrating that these characteristic cell behaviors are generated by SLUG through the downstream factors, MMP9, MMP14, CXCL12 and E-cadherin.

During early-postnatal pituitary development, the anterior pituitary undergoes a substantial growth wave with the appearance and proliferation of cells. As some S100β-positive cells have been hypothesized to be a pituitary cell resource acting as postnatal stem cells (Yoshida et al. 2009, 2011; Higuchi et al. 2014), they might differentiate into hormone-producing cells. However, the present study also revealed the mechanism of self-duplication in S100β-positive cells in the developing anterior lobe. These findings contribute to a deeper understanding of the histogenesis of the anterior pituitary gland with age.

References

Allaerts W, Vankelecom H (2005) History and perspectives of pituitary folliculo-stellate cell research. Eur J Endocrinol 153:1–12

Allaerts W, Fluitsma DM, Hoefsmit EC, Jeucken PH, Morreau H, Bosman FT, Drexhage HA (1996) Immunohistochemical, morphological and ultrastructural resemblance between dendritic cells and folliculo-stellate cells in normal human and rat anterior pituitaries. J Neuroendocrinol 8:17–29

Aybar MJ, Nieto MA, Mayor R (2003) Snail precedes slug in the genetic cascade required for the specification and migration of the *Xenopus* neural crest. Development 130:483–494

Batlle E, Sancho E, Francí C, Domínguez D, Monfar M, Baulida J, García De Herreros A (2000) The transcription factor snail is a repressor of E-cadherin gene expression in epithelial tumour cells. Nat Cell Biol 2:84–89

Bolos V, Peinado H, Perez-Moreno MA, Fraga MF, Esteller M, Cano A (2003) The transcription factor slug represses E-cadherin expression and induces epithelial to mesenchymal transitions: a comparison with snail and E47 repressors. J Cell Sci 116:499–511

Higuchi M, Kanno N, Yoshida S, Ueharu H, Chen M, Yako H, Shibuya S, Sekita M, Tsuda M, Mitsuishi H, Kato T, Kato Y (2014) GFP-expressing S100β-positive cells of the rat anterior pituitary differentiate into hormone-producing cells. Cell Tissue Res 357:767–779

Höfler H, Denk H, Walter GF (1984) Immunohistochemical demonstration of cytokeratins in endocrine cells of the human pituitary gland and in pituitary adenomas. Virchows Arch A Pathol Anat Histopathol 404:359–368

Horacek MJ, Thompson JC, Dada MO, Terracio L (1993) The extracellular matrix components laminin, fibronectin, and collagen IV are present among the epithelial cells forming Rathke's pouch. Acta Anat (Basel) 147:69–74

Horiguchi K, Kikuchi M, Kusumoto K, Fujiwara K, Kouki T, Kawanishi K, Yashiro T (2010) Living-cell imaging of transgenic rat anterior pituitary cells in primary culture reveals novel characteristics of folliculo-stellate cells. J Endocrinol 204:115–123

Horiguchi K, Kouki T, Fujiwara K, Kikuchi M, Yashiro T (2011a) The extracellular matrix component laminin promotes gap junction formation in the rat anterior pituitary gland. J Endocrinol 208:225–232

Horiguchi K, Fujiwara K, Ilmiawati C, Kikuchi M, Tsukada T, Yashiro T (2011b) Caveolin 3-mediated integrin β1 signaling is required for the proliferation of folliculo-stellate cells in rat anterior pituitary gland under the influence of extracellular matrix. J Endocrinol 211:29–36

Horiguchi K, Ilmiawati C, Fujiwara K, Tsukada T, Kikuchi M, Yashiro T (2012) Expression of chemokine CXCL12 and its receptor CXCR4 in folliculostellate (FS) cells of the rat anterior pituitary gland: the

CXCL12/CXCR4 axis induces interconnection of FS cells. Endocrinology 153:1717–1724

Horiguchi K, Fujiwara K, Yoshida S, Higuchi M, Tsukada T, Kanno N, Yashiro T, Tateno K, Ohsako S, Kato T, Kato Y (2014) Isolation of dendritic cell-like S100β-positive cells in rat anterior pituitary gland. Cell Tissue Res 357:301–308

Ilmiawati C, Horiguchi K, Fujiwara K, Yashiro T (2012) Matrix metalloproteinase-9 expression in folliculostellate cells of rat anterior pituitary gland. J Endocrinol 212:363–370

Inoue K, Couch EF, Takano K, Ogawa S (1999) The structure and function of folliculo-stellate cells in the anterior pituitary gland. Arch Histol Cytol 62:205–218

Itakura E, Odaira K, Yokoyama K, Osuna M, Hara T, Inoue K (2007) Generation of transgenic rats expressing green fluorescent protein in S-100beta-producing pituitary folliculo-stellate cells and brain astrocytes. Endocrinology 148:1518–1523

Jordà M, Olmeda D, Vinyals A, Valero E, Cubillo E, Llorens A, Cano A, Fabra A (2005) Upregulation of MMP-9 in MDCK epithelial cell line in response to expression of the Snail transcription factor. J Cell Sci 118:3371–3385

Joseph MJ, Dangi-Garimella S, Shields MA, Diamond ME, Sun L, Koblinski JE, Munshi HG (2009) Slug is a downstream mediator of transforming growth factor-beta1-induced matrix metalloproteinase-9 expression and invasion of oral cancer cells. J Cell Biochem 108:726–736

Kikuchi M, Yatabe M, Fujiwara K, Takigami S, Sakamoto A, Soji T, Yashiro T (2006) Distinctive localization of N- and E-cadherins in rat anterior pituitary gland. Anat Rec A Discov Mol Cell Evol Biol 288:1183–1189

Moore BW (1965) A soluble protein characteristic of the nervous system. Biochem Biophys Res Commun 19:739–744

Nieto MA (2002) The snail superfamily of zinc-finger transcription factors. Nat Rev Mol Cell Biol 3:155–166

Nieto MA, Sargent MG, Wilkinson DG, Cooke J (1994) Control of cell behavior during vertebrate development by Slug, a zinc finger gene. Science 264:835–839

Piva R, Manferdini C, Lambertini E, Torreggiani E, Penolazzi L, Gambari R, Pastore A, Pelucchi S, Gabusi E, Piacentini A, Filardo G, Facchini A, Lisignoli G (2011) Slug contributes to the regulation of CXCL12 expression in human osteoblasts. Exp Cell Res 317:1159–1168

Ramadhani D, Tsukada T, Fujiwara K, Azuma M, Kikuchi M, Yashiro T (2014) Change in laminin chain expression in pre- and postnatal rat pituitary gland. Acta Histochem Cytochem 47:231–247

Sanchez-Martin M, Perez-Losada J, Rodriguez-Garcia A, Gonzalez-Sanchez B, Korf BR, Kuster W, Moss C, Spritz RA, Sánchez-García I (2003) Deletion of the SLUG (SNAI2) gene results in human piebaldism. Am J Med Genet A 122:125–132

Sefton M, Sánchez S, Nieto MA (1998) Conserved and divergent roles for members of the Snail family of transcription factors in the chick and mouse embryo. Development 125:3111–3121

Shields MA, Krantz SB, Bentrem DJ, Dangi-Garimella S, Munshi HG (2012) Interplay between β1-integrin and Rho signaling regulates differential scattering and motility of pancreatic cancer cells by snail and slug proteins. J Biol Chem 287:6218–6229

Soji T, Sirasawa N, Kurono C, Yashiro T, Herbert DC (1994) Immunohistochemical study of the post-natal development of the folliculo-stellate cells in the rat anterior pituitary gland. Tissue Cell 26:1–8

Soji T, Mabuchi Y, Kurono C, Herbert DC (1997) Folliculo-stellate cells and intercellular communication within the rat anterior pituitary gland. Microsc Res Tech 39:138–149

Tachibana O, Yamashima T (1988) Immunohistochemical study of folliculo-stellate cells in human pituitary adenomas. Acta Neuropathol 76:458–464

Uygur B, Wu WS (2011) SLUG promotes prostate cancer cell migration and invasion via CXCR4/CXCL12 axis. Mol Cancer 10:139

Yoshida S, Kato T, Susa T, Cai LY, Nakayama M, Kato Y (2009) PROP1 coexists with SOX2 and induces PIT1-commitment cells. Biochem Biophys Res Commun 385:11–15

Yoshida S, Kato T, Yako H, Susa T, Cai LY, Osuna M, Inoue K, Kato Y (2011) Significant quantitative and qualitative transition in pituitary stem / progenitor cells occurs during the postnatal development of the rat anterior pituitary. J Neuroendocrinol 23:933–943

Yoshida S, Kato T, Higuchi M, Yako H, Chen M, Kanno N, Ueharu H, Kato Y (2013) Rapid transition of NESTIN-expressing dividing cells from PROP1-positive to PIT1-positive advances prenatal pituitary development. J Neuroendocrinol 25:779–791